Impact of TE-MHD Coupling on Cell Performance

Louis Bugnion[1], René von Kaenel[2]
1. Head of modelling
2. CEO
KAN-NAK SA, CH-3960 Sierre, Switzerland
Corresponding author: louis.bugnion@kannak.ch

Abstract

Metal velocity and metal upheaval have a significant effect on the temperature field in an aluminium reduction cell, and consequently on the ledge shape which in turn influences current density and metal velocity. This so-called coupling between thermal-electric (TE) and magneto-hydrodynamic (MHD) effects has an impact on the performance of the cell and evolves with increasing line amperage. Results of TE-MHD calculations on a full 3D cell show the importance of this coupling on the variable fields. Scenarios at different amperages are compared as well as the scenario in which the ledge variations induced by the coupling are compensated for by adjusting the heat extraction around the cell. The numerical model used in this study solves the full heat equation including convection and turbulent conductivity of the liquid bath and metal. The opportunity to mitigate MHD effects and/or compensate them thermally is discussed in the perspective of ledge control and cell performance.

Keywords: Modelling, TE-MHD coupling, Temperature field, Ledge shape.

1. Introduction

The modelling of the TE-MHD coupling in an aluminium reduction cell has been tackled in different ways over the years. Early attempts [1] resorted to weak coupling to model the heat flux at the liquid bath-ledge and metal-ledge interfaces. Velocity dependent heat transfer coefficients were used to account for the convection of heat. Variation of the ledge profile along the cell sides was limited and had a marginal impact on the velocity field. Some years later, a similar approach to the present one was implemented in the Alucell software [2], solving the transient heat equation formulated in enthalpy. The full 3D cell problem requires to solve Maxwell equations for the electrical potential and magnetic induction, Navier-Stokes equations for the pressure and velocity and the heat equation for the temperature. It makes a total of 9 unknown scalar fields complemented by boundary and interface conditions. The in-house MONA software [3], specialized in the modelling of the aluminium reduction cell, solves the 3D strong coupling of the 9 unknowns and predicts the ledge shape and metal surface simultaneously. MONA software can also be used to compute the diffusion of alumina in the bath and the MHD stability of the cell (growth factor of metal pad oscillations).

In the present work, the stationary heat equation – Equation (1) – formulated in enthalpy – Equation (2) – and Robin non-linear boundary condition – Equation (3) – are solved by means of the Finite-Element (FE) Method.

The first term on the left in Equation (1) is the heat advection term (TE-MHD coupling) whereas the second term is the heat diffusion term. The term on the right is the heat source term. Numerical oscillations caused by the convection term are prevented using a decentering SUPG (Streamline Upwind Petrov-Galerkin) technique with shock-capturing parameters [4].

$$\boldsymbol{v} \cdot \boldsymbol{\nabla} H - div(\lambda \boldsymbol{\nabla} \mathrm{T}) = q \qquad\qquad (1)$$

$$H(T) = \rho C_p T + \rho L f_l \qquad (2)$$

$$\lambda \boldsymbol{\nabla} T \cdot \boldsymbol{n} = \alpha(T)(T - T_\infty) \qquad (3)$$

where:

v	velocity, m/s
H	enthalpy, J/m^3
λ	thermal conductivity, W/(m·K)
T	temperature, K
q	Joule heat source, W/m^3
ρ	density, kg/m^3
C$_p$	specific heat, J/(kg·K)
L	latent heat of fusion, J/kg
f$_l$	liquid fraction
n	unit vector normal to boundary
α	heat transfer coefficient, W/(m^2·K).

As in reference [2], the FE mesh is refined in the bath and metal parts where the solidification takes place (see Figure 1). For the calculation of the magnetic induction, both the studied and neighboring cells are modeled in full 3D whereas cells further away in the potline(s) are modelled by means of 3D wireframe elements. Temperature dependent material properties are considered while contact resistances and heat transfer coefficients at mesh boundaries (*i.e.*, free surfaces) are calibrated.

Heat transfer coefficients applied to the external surfaces of busbars, collector bars (outside the shell), shell bottom, shell sides and anode cover are calibrated separately whereas in reference [2], the heat transfer coefficient of shell sides is further differentiated between upstream (US) and downstream (DS) sides and corners. In liquid parts, turbulent viscosity, and thermal conductivity dependent on velocity gradients are included.
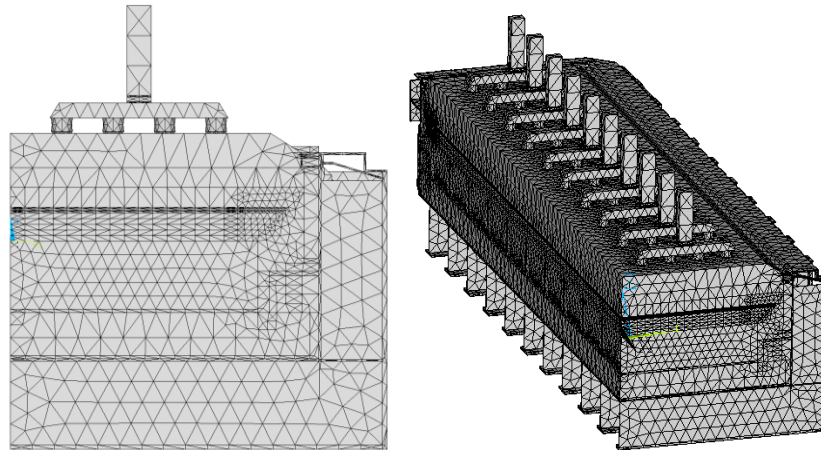

Figure 1. FE mesh of a typical cell quarter without busbars. Complete pot geometry is obtained by reflection.

2.   Numerical Study

The purpose of this study is to demonstrate the effect of metal velocity and metal upheaval on the temperature field and thus on the ledge shape which is critical for cell operation and cell life. Three cases are presented: the reference cell operated at 360 kA, the impact of increasing current

to 380 kA and the impact of adjusted heat extraction. To ease comparison, plots of the three cases are grouped in the same figure.

2.1 Reference Case

Calculations are performed on an AP3X technology pot with forced convection. The reference case at 360 kA is calibrated based on temperature and voltage measurements. The anode-to-cathode distance (ACD) is adjusted to achieve a good ledge protection of the cell lining.

The ledge shape at the cathode surface (view of the metal pad bottom) is shown in Figure 2 a) and the metal velocity field 10 cm above cathode surface level is shown in Figure 3 a), where it can be seen that two main vortices flowing in opposite directions characterize the velocity field.

a)   Reference case, 360 kA
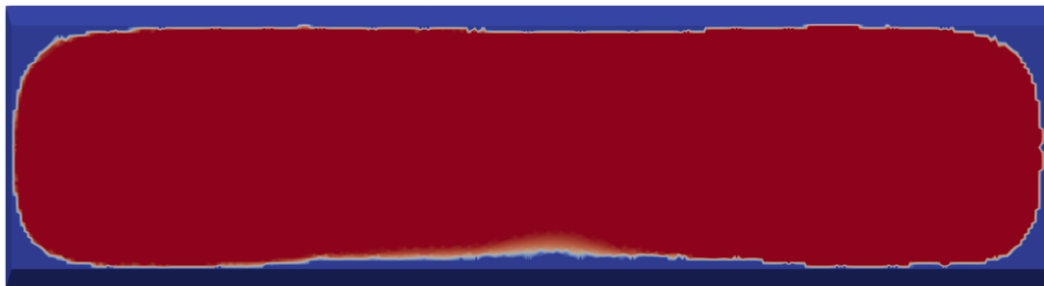
b)   Increased amperage case, 380 kA

c)   Adjusted heat extraction case, 360 kA

Figure 2. Ledge shape (blue) at cathode surface (view of the metal pad bottom), where potline current flows from the bottom (US) to the top (DS) of the page.

The centers of these vortices define regions with low velocity and higher bath/metal temperature (see Figure 4). The heat generated in these regions is not advected outwards (only diffused). In the cell center, between the main vortices, a cooler region shows low velocity directed from upstream side (colder) to downstream side (warmer) in such a way that bath/metal is heated up while flowing across the cell.

In the center of the upstream side, the velocity is parallel to the temperature gradient (ledge has a lower temperature than bath/metal) yielding a positive advection term on the left of Equation (1), which corresponds to a heat sink (negative if moved to the right of the equation). As a result, a longer ledge toe builds up at that location.

a) Reference case, 360 kA, average velocity 7.5 cm/s, max 19.1 cm/s

b) Increased amperage case, 380 kA, average velocity 8.1 cm/s, max 20.5 cm/s

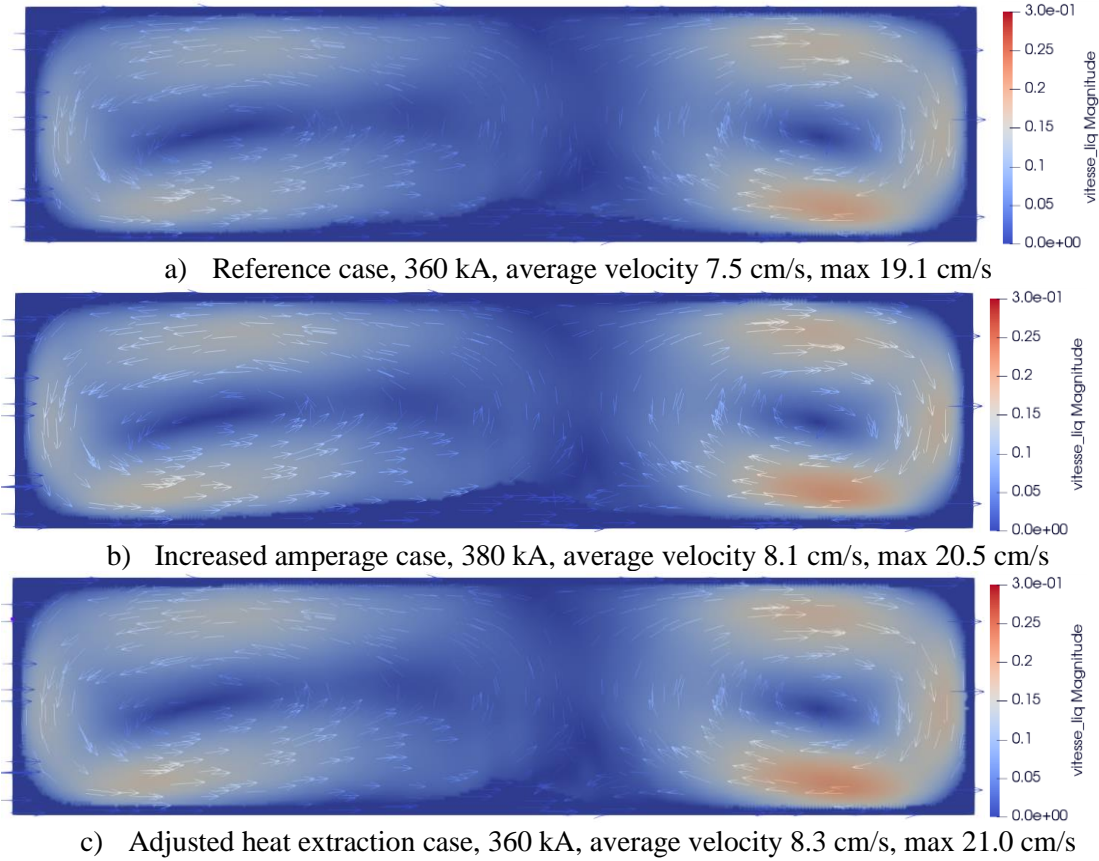c) Adjusted heat extraction case, 360 kA, average velocity 8.3 cm/s, max 21.0 cm/s

Figure 3. Metal velocity field 10 cm above cathode surface level, [m/s], where potline current flows from the bottom (US) to the top (DS) of the page. Velocity magnitude shown in color while arrows indicate horizontal components.
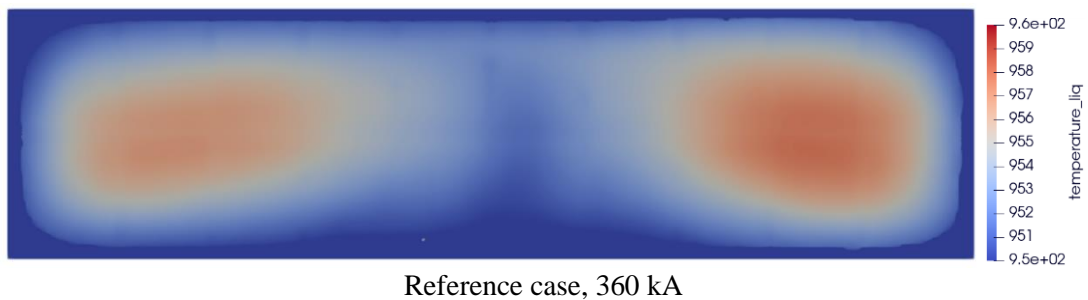

Reference case, 360 kA

Figure 4. Bath temperature field 20 cm above cathode surface level, [°C], where potline current flows from the bottom (US) to the top (DS) of the page. Liquidus temperature is 953°C and maximum bath temperature is 961°C.

The ledge acts as a thermal insulator and the shell temperature is consequently lower at the center of the upstream side – see Figure 5 a). Likewise, a longer ledge toe reduces the cathode conductive surface leading to higher current density at its extremity. High current density at the cathode surface (meaning horizontal currents in metal) is detrimental to cell stability and cell life (electro-

erosion). The collector bar current distribution is also affected (less current at the center of the upstream side).

In contrast, the center of the downstream side benefits from a negative advection term (heat source) limiting the ledge thickness even though the temperature gradient is low. The long sides at the location of the vortices show thinner ledge mainly due to the diffusion term in Equation (1) (large temperature gradients oriented inwards and velocity gradients enhancing the turbulent thermal conductivity). Advection is small since velocity is perpendicular to temperature gradients.

Figure 5 a) shows the computed shell temperature on the long sides at bath-metal interface level. The maximum predicted difference in temperature between upstream and downstream sides is 30°C in the center of the long sides. On the other hand, measurements performed on 10 cells (see Figure 6) show a difference of 50°C. The discrepancy between empirical and numerical results may either relate to thinner ledge shape on the downstream side of the measured cells (we have adjusted the ACD to achieve a good ledge protection everywhere) or to different ledge shape due to erosion of the ramming paste layer (calculations are performed on a new cell geometry).
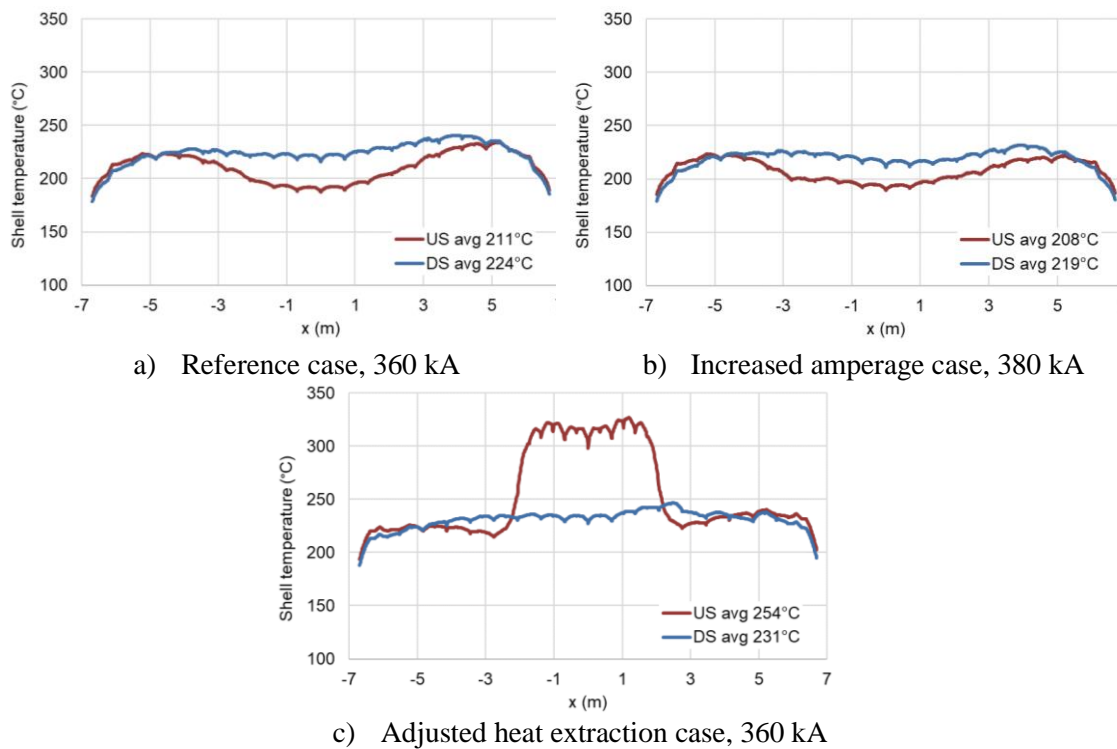
a) Reference case, 360 kA   b) Increased amperage case, 380 kA

c) Adjusted heat extraction case, 360 kA

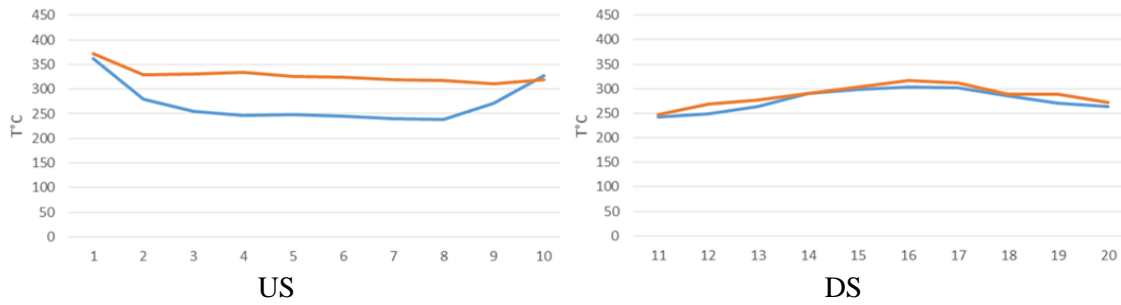**Figure 5. Shell temperature profiles at metal level as a function of sidewall length.**

Figure 6. Measured average maximum shell temperature above pairs of collector bars (10 cells). Blue lines indicate the reference case while orange ones, the adjusted heat extraction case.

The asymmetry in metal upheaval between upstream and downstream sides (around 3 cm, see Figure 7) also contributes to the temperature field, higher metal level enhancing heat transfer to the sides. For this technology, the impact of metal upheaval is lower compared to the one of velocity and accounts for less than 10 °C in the shell temperature asymmetry.
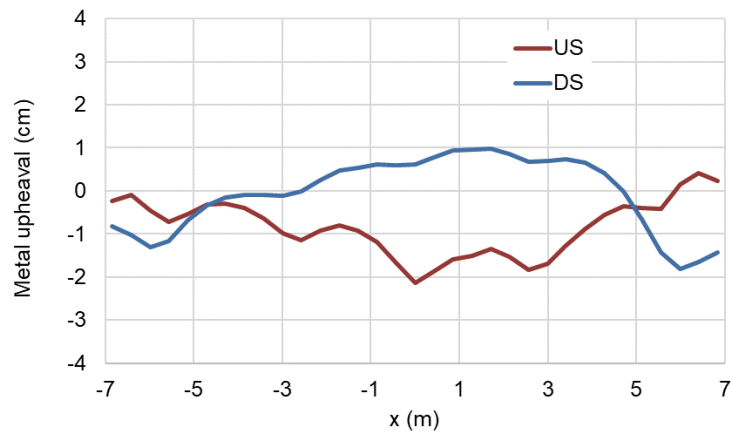

Figure 7. Reference case, 360 kA, metal upheaval profiles on long sides.

2.2 Increased Amperage Case

A second case at 380 kA is presented to highlight the impact of the amperage on the thermal status of the cell. The maximum bath temperature is marginally increased (+ 1°C). The ACD has been decreased to achieve a good ledge protection (internal heat generation is slightly higher though). The phenomenon seen at 360 kA also takes place, resulting in a longer ledge toe in the center of the upstream side. Higher velocity values – see Figure 3 b) – slightly increase the longitudinal distance over which the ledge toe is visible – see Figure 2 b. It means that the region over which convection is significant has been extended.

2.3 Adjusted Heat Extraction Case

The third case simulates a test performed on 10 AP3X technology cells. Heat extraction was adjusted to smoothen shell temperature variations along the sidewalls themselves as well as between upstream and downstream sides. The objective was to reduce the total heat extraction and thus cell voltage while making the ledge shape more uniform. Figure 6 shows two sets of measured maximum shell temperature profiles over the long sides (each set is the average of the 10 profiles). Blue lines show reference temperature profiles whereas orange lines show temperature profiles after heat extraction was adjusted.

The computed scenario – see Figures 2 c), 3 c) and 5 c) – goes beyond the actual test since heat extraction is adjusted to smoothen not the temperature but the ledge variations along the sidewalls themselves as well as between upstream and downstream sides. The results show that the thicker ledge region on the upstream side is significantly reduced. Interestingly, the corresponding shell temperature profiles are not uniform, see Figure 5 c). To compensate for the positive convection term (heat sink) on the upstream side, higher temperatures are needed on the shell sidewall to achieve a thinner ledge. It indicates that the ledge shape of the cells documented in Figure 6 was made more uniform but only partially.

The smoother ledge shape leads to higher metal velocity in the vicinity of the US sidewall center (average and maximum velocities are higher, see Figure 3). It agrees with our calculations showing that velocity is higher if there is no ledge.

3.   Conclusion

Ledge shape is not monitored on a routine basis in aluminium smelters but is indirectly followed up through shell temperature measurements and Si content analysis of the tapped metal. Ledge is essential to pot operation as it protects the cell lining from bath corrosion, but it may destabilize the cell if it freezes the cathode surface. The modelling tools used in this study help at better understanding the interaction between the temperature of the liquid parts and their velocity distribution. The impact of amperage on the cell status is highlighted as well as the possibility to adjust heat extraction around the cell to make the ledge shape more uniform. Just as metal velocity disturbs the cell, enhancing MHD instability and metal reoxidation, its pattern affects the temperature field and determines the ledge shape. Reducing high metal velocity through operation (metal level) and/or by cell design (anode dimensions, cathode and busbars designs) will be beneficial to the cell. Adjusting heat extraction around the cell (shell design, forced convection) is also an option to counteract the effect of MHD on the thermal state of the cell. After testing many numerical schemes, the decentering SUPG technique with shock-capturing parameters [4] proved to be a robust solution for predicting the ledge shape in presence of TE-MHD effects. It is presently implemented in the MONA software [3].

4.   References

1.   Marc Dupuis and Valdis Bojarevics, Weakly coupled thermo-electric and MHD mathematical models of an aluminium electrolysis cell, *Light Metals* 2005, 449-454.
2.   S. Langlois *et al.*, 3D coupled MHD and thermo-electrical modelling applied to AP technology pots, *Light Metals* 2015, 771-775.
3.   MONA: Thermal and Magnetohydrodynamic Software, http://kannak.ch/PDF/2004-MONA-Software.pdf (Accessed on 21 August 2023).
4.   V. John, P. Knobloch, On spurious oscillations at layers diminishing (SOLD) methods for convection diffusion equations, Part I A review *Computer Methods in Applied Mechanics and Engineering.* 196 (2007), 2197-2215.